



Surface modification of graphite encapsulated iron nanoparticles by plasma processing[☆]

Teguh E. Saraswati, Takafumi Matsuda, Akihisa Ogino, Masaaki Nagatsu^{*}

Graduate School of Science and Technology, Shizuoka University, 3-5-1, Johoku, Naka-ku, Hamamatsu 432-8561, Japan

ARTICLE INFO

Available online 19 January 2011

Keywords:

Graphite
Iron nanoparticles
RF plasma processing
Ammonia plasma

ABSTRACT

The graphite encapsulated iron nanoparticles were fabricated by using arc discharge method. The synthesized nanoparticles were pre-treated by an inductively-coupled RF Ar plasma and then post-treated by NH₃ plasma under various gas pressures and treatment times. Analyses of XPS spectra have been carried out to study the effect of the plasma treatment on the surface modification of nitrogen-containing groups. The morphological changes of the particles surface by plasma treatment have also been analyzed by using HR-TEM. Present results show that the highest values of N/C atomic ratio of 5.4% is obtained by applying 10 min of Ar plasma pre-treatment and 2 min of NH₃ plasma post-treatment conducted in RF power of 80 W and gas pressure of 50 Pa.

© 2011 Elsevier B.V. All rights reserved.

1. Introduction

Iron nanoparticles have many great interests in potential to bio-application such as drug delivery system, hyperthermia treatments, magnetic resonance imaging contrast enhancement, etc [1–8]. The carbon-encapsulated metal nanoparticles were first synthesized as LaC in 1993 by Ruoff et al. [9]. So far, these particles have been commonly produced by conventional arc discharge [10–15], modified arc discharge [16,17], chemical vapor deposition (CVD), combustion, laser synthesis, ion beam sputtering [18], and annealing microporous carbon or diamond with metal nanoparticles [19]. Carbon coating of the magnetic nanoparticles can leave the toxicity out without detracting their magnetic properties. Moreover, the carbon coating not only stabilize the nanoparticles but can also be used for further functionalization, such as addition of the therapeutic agent, targeting agent or fluorophore, depending on the purposes.

Among various functional groups for bio-application, the introduction of amino groups composed of primary amines to the particles surface achieves enhanced wettability and improves its adhesion. Some early work by I.H. Loh et al. reports the use of ammonia plasma, nitrogen and nitrogen/hydrogen mixtures on carbon black [20]. Recently, there are also several other papers studying about the amino functionalization for carbon nanotubes [21,22], amorphous carbon sheet [23], nanocrystalline diamond [24,25], carbon nanoparticles [26], etc. However, this modification has not been deeply studied on carbon-encapsulated

magnetic nanoparticles. In fact very few information can be found on the topic of graphite encapsulated iron nanoparticles related to the plasma surface treatment in order to introduce nitrogen-containing group functionalities, such as amino group.

In this study, we mainly functionalize the graphite encapsulated iron nanoparticles using Ar and NH₃ plasma performed by an inductively-coupled radio frequency plasma. X-ray diffraction (XRD), X-ray photoelectron spectroscopy (XPS), high resolution-transmission electron microscopy (HR-TEM), and energy dispersive X-ray spectroscopy (EDS) elemental mapping were used to characterize and analyze the results.

2. Experimental details

The graphite encapsulated iron particles were prepared by using arc discharge method refers to Refs. [14,15]. The arc discharge was generated by applying a dc current of 150–200 A at about 20 V voltage between anode and cathode. Graphite electrodes molded with Fe₂O₃ powder by using graphibond-551R was used as anode. In the other side, graphite rod was used as cathode. Both of those electrodes were set with distance as near as possible in a stainless-steel vacuum chamber with 200 mm diameter. The chamber was evacuated to around 1 Pa by a rotary pump. A mixture gas of He:CH₄ with ratio 4:1 was flown to the chamber until the pressure reached 1.3×10^4 Pa. Then, carrying a high current between the electrodes will provide lots of composite powders. The powders were directly deposited on silicon substrates set inside the chamber. In order to obtain crystallographic characteristics, X-ray diffraction (XRD) measurements were performed with a RIGAKU RINT Ultima. For structural characterization, observation using HR-TEM was performed by using a JEM-2100F equipped CCD camera. The TEM sample was prepared by dispersing the nanoparticles

[☆] Presented at NDNC 2010, the 4th International Conference on New Diamond and Nano Carbons, Suzhou, China.

^{*} Corresponding author.

E-mail address: tmnagat@ipc.shizuoka.ac.jp (M. Nagatsu).

in ethanol and dropped onto the carbon grid. The TEM observation was conducted at an accelerating voltage of 200 kV.

Following the nanoparticle synthesis step, the nanoparticles are treated by using an inductively-coupled radio frequency plasma device. The schematic view of the chamber is shown in Fig. 1. The chamber is 200 mm both in diameter and height. The water-cooling copper pipe helical antenna, 100 mm in coil diameter and 20 mm in pipe diameter, was coupled to an RF power generator at 13.56 MHz via a matching net-work. Typical input RF power was about 80 W.

Samples were set in the glass dish placed on the stage inside the chamber. There are two-steps plasma treatment performed here. In the first step, pre-treatment was performed with Ar plasma and subsequently NH_3 gas plasma was used as the post-treatment to introduce the amino groups. The period time of plasma pre-treatment was performed for 10 min, while the period time of the post-treatment was varied to 2, 5 and 10 min. During the experiment, the gas pressure was varied as 5, 10 and 50 Pa at a fixed gas flow rate of 50 sccm. After the plasma treatment, the treated samples are characterized by using XPS performed by Shimadzu ESCA-3400 with Mg K α X-Ray source and EDS elemental mapping performed by a JEM-2100F.

3. Results and discussion

The graphite encapsulated iron nanoparticles are successfully synthesized by arc discharge method. First, it is confirmed that the synthesized powders have a magnetic property, as shown in Fig. 2a. The powders stirred in the purified water in the bottle are attracted by a permanent magnet, even when the magnet was located far from the bottle. In order to confirm their phase and structural characterization, XRD and HR-TEM analysis was carried out. The XRD profile presented in Fig. 2b shows the presence of graphitic carbon (JCPDS 00-056-0159), crystallized α -Fe (JCPDS 00-006-0696), iron carbides (Fe_3C) (JCPDS 01-072-1110) and iron oxide (Fe_2O_3) (JCPDS 00-033-0664). Typical TEM image of graphite encapsulated iron nanoparticles taken in high magnification is presented in Fig. 2c. The diameters of particles are mainly around 10–50 nm in size measured from the outmost graphene layer. The spacing of the graphene layers is about 0.34 nm.

To investigate the effect of chemical modification on the plasma-treated surfaces by Ar and NH_3 plasma, XPS measurements were

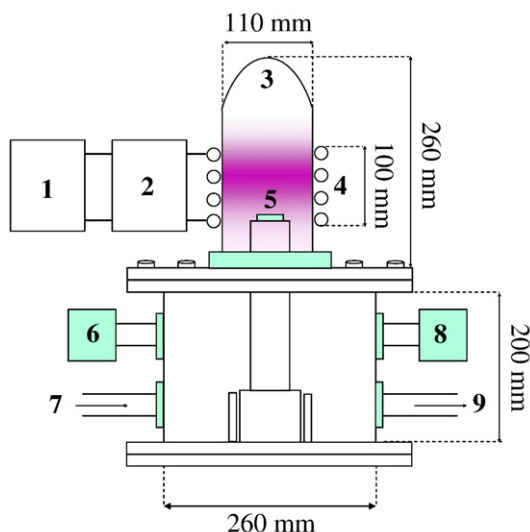


Fig. 1. Schematic view of experimental setup of inductively-coupled RF plasma. (1) RF powers supply, (2) Matching box, (3) Glass jar, (4) Copper coil connected to the water-cooling system, (5) Sample place, (6) Pressure gauge, (7) Gas inlet, (8) Leaking valve, (9) Gas outlet connected to the turbo and rotary pump.

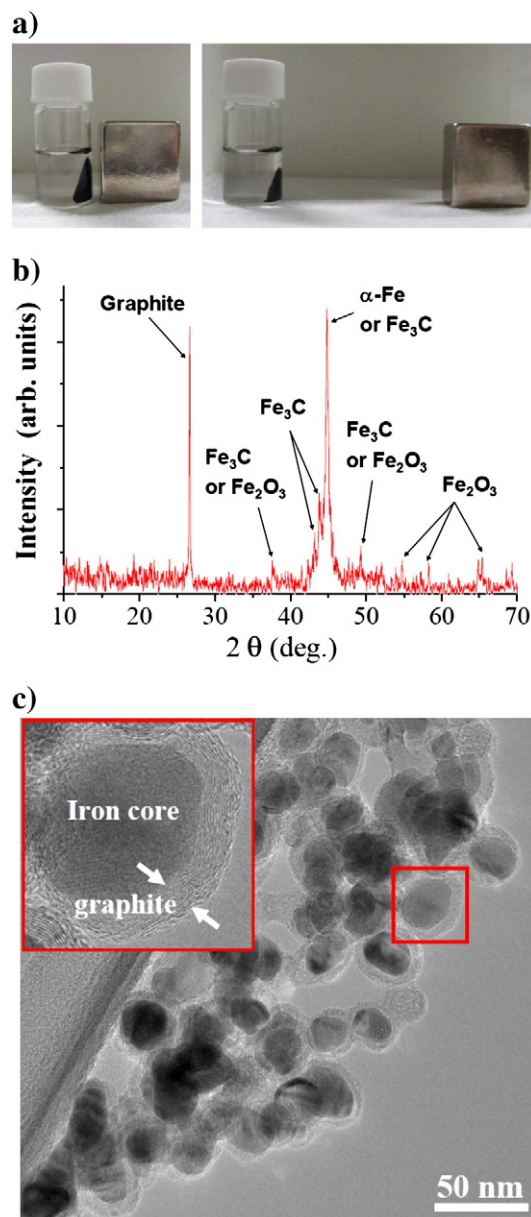


Fig. 2. (a) The synthesized particles (diluted in water) show the attractive interaction with magnet in close and far distance; (b) XRD profile of pristine sample of graphite encapsulated iron nanoparticles; (c) HR-TEM images of graphite encapsulated iron nanoparticles.

carried out. The relative compositions of C 1s, N 1s, O 1s and Fe 2p, and atomic ratios of O/C and N/C of the samples before and after plasma treatment under different plasma conditions are listed in Table 1. The experimental results show that the relative composition of C 1s decreased after plasma treatment due to the ion bombardment of Ar plasma pre-treatment. With the Ar plasma pre-treatment, many free carbon bonding are expected to be created in the outmost of graphene layer and then react directly with NH_3 plasma to introduce the amino group on the particle surface.

Comparing to the untreated sample, O/C atomic ratio of the samples after plasma treatment increased. The increase of O/C atomic ratio may be resulted from the following processes. First, carbon radicals are formed in the outermost shell of graphene layers by Ar plasma pre-treatment and NH_3 plasma post-treatment, where the sample surfaces are bombarded by electrons and ions and provide graphene layers with graphite bonding that would be lopped off to form carbon radicals. These radicals then can easily connect with

Table 1

Atomic composition of C 1s, O 1s, N 1s and Fe 2p peaks and atomic ratio of O/C and N/C taken from the XPS spectra before and after plasma treatment under various plasma conditions.

Sample	Treatment period (min)		Atomic composition (%)						Atomic ratio (%)	
	Pre-treatment	Post-treatment	C 1s	O 1s	N 1s	Fe 2p 3/2	Fe 2p 1/2	O/C	N/C	
Untreated	–	–	87.91	10.68	0.00	0.82	0.59	12.15	0.00	
80 W, 5 Pa	10	2	76.02	19.01	1.15	2.26	1.56	25.01	1.51	
	10	5	74.62	18.18	1.11	3.31	2.78	24.36	1.49	
	10	10	85.50	11.22	0.94	1.43	0.90	13.12	1.10	
80 W, 10 Pa	10	2	81.02	14.72	1.02	2.24	1.01	18.17	1.26	
	10	5	80.15	16.05	1.73	1.67	0.40	20.02	2.16	
	10	10	76.93	16.12	3.51	1.58	1.87	20.95	4.56	
80 W, 50 Pa	10	2	81.30	12.14	4.40	1.75	0.40	14.93	5.41	
	10	5	82.13	12.48	1.90	2.44	1.05	15.20	2.31	
	10	10	82.91	12.71	1.08	2.19	1.10	15.33	1.30	

Plasma condition: Ar and NH₃ gas flow was kept on 50 sccm.

oxygen after opening to the atmosphere, which may result in the increasing of O/C atomic ratio.

The increase of N/C atomic ration indicates the formation of some nitrogen-containing groups on the outmost of graphene layers by NH₃ plasma treatment. As for the treatment time, in the case of plasma condition at 5 Pa, the post-treatment time does not give a significant influence to the N/C atomic ratio. While the plasma condition at 10 Pa, the increase of post-treatment time will also make an increase their N/C atomic ratio. On the other hand, in the case of plasma condition at 50 Pa, the result is contrary. The highest enrichment of nitrogen-containing functionalities shown from N/C atomic ratio was obtained in the case of 2 min NH₃ plasma post-treatment at 50 Pa. The nitrogen percentage decreased when the period time of post-treatment is longer than 2 min. This indicates that in the case of treatment in 50 Pa, NH₃ plasma post-treatment time longer than 2 min is too long because the bound amino groups would be released by the electrons and ions existing in NH₃ plasma. On the other hand, it is expected that opposite phenomena occur for plasma treatment performed in 10 Pa. The treatment times of 2 and 5 min at 10 Pa are still not optimum enough for linking nitrogen-containing groups.

As shown in Fig. 3, the XPS spectra of both (i) untreated and (ii) treated sample of C 1s, O 1s, N 1s and Fe 2p regions are respectively

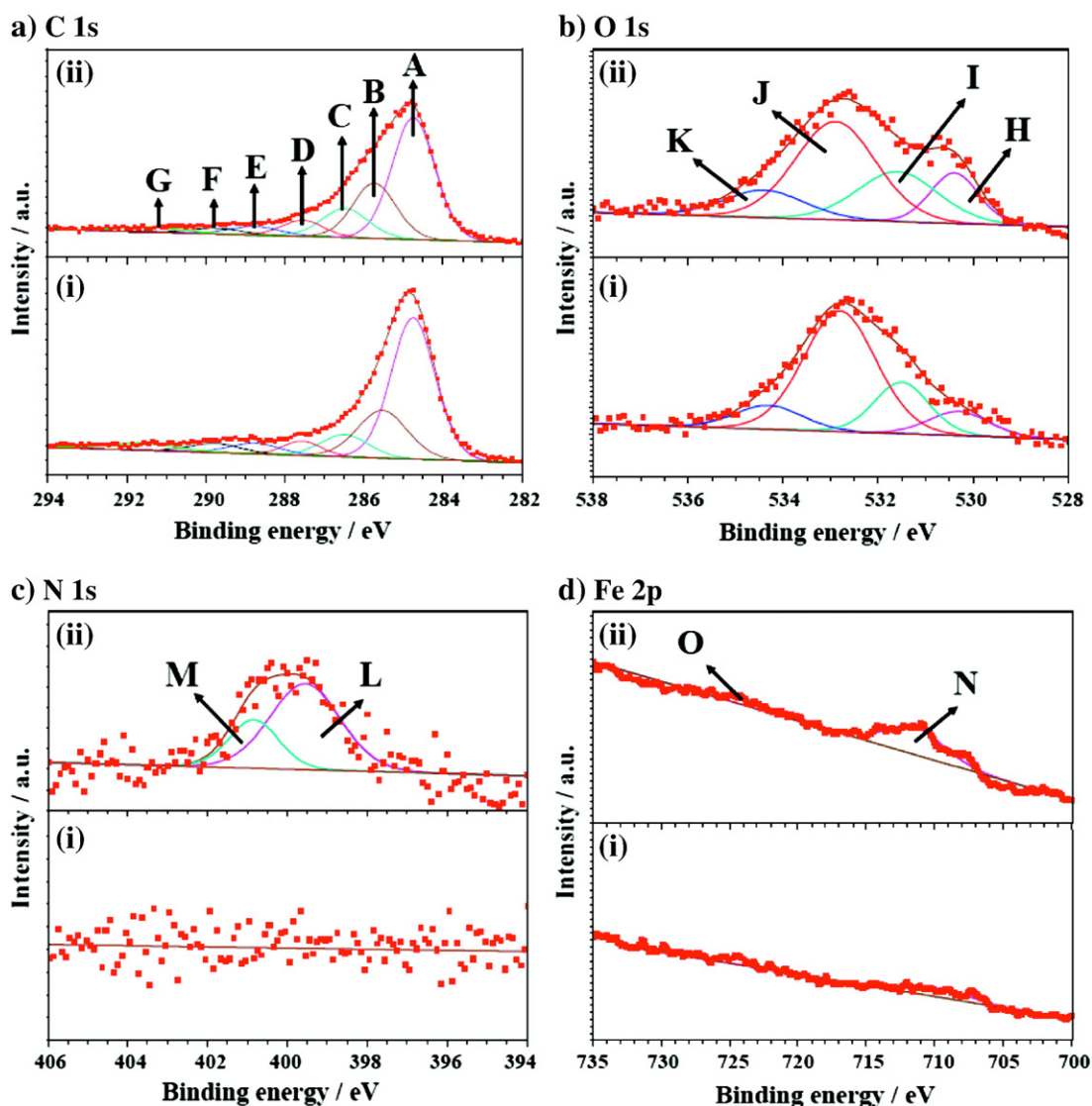


Fig. 3. XPS spectra in C 1s (a), O 1s (b), N 1s (c) and Fe 2p (d) region before (i) and after (ii) plasma treatment with condition: 10 min of Ar plasma pre-treatment followed by with 2 min of NH₃ plasma post-treatment performed at 80 W of RF power and 50 Pa of gas pressure.

shown in Fig. 3a, b, c, and d, respectively. The treated sample shown in Fig. 3 corresponds to the treated sample with the highest enrichment of nitrogen-containing groups (80 W, 50 Pa, 10 min of pre-treatment and 2 min of post-treatment). Each of the spectra was deconvoluted to several possible peaks based on the Refs. [21,27–37]. The C 1s spectrum shown in Fig. 3a consists of several peaks, that are, graphitic carbon peak of C–C sp^2 at around 284.75 ± 0.01 eV (denoted by A) [35]; C–C sp^3 at around 285.63 ± 0.10 eV (B) [35]; carbon present in C–O and C–N at around 286.49 ± 0.01 eV (C); carbon present in C O at around 287.55 ± 0.01 eV (D); carbon present in O C–O and O C–N at around 288.75 ± 0.01 eV (E); carbon present in carbonate groups ($-O_2C O$) at around 289.75 ± 0.01 eV (F) and typical $\pi-\pi^*$ shake-up satellite at around 291.49 ± 0.10 eV (G) [21,27,32,33,36,37]. The O 1s spectra shown in Fig. 3b fitted to four component peaks: that corresponds to the lattice oxygen (O^{2-} in FeO) at around 530.52 ± 0.14 eV (H) [28,30,31]; C O groups at around 532.09 ± 0.09 eV (I); C–OH and or C–O–C groups at around 533.23 ± 0.14 eV (J) and O C–O groups at around 534.34 ± 0.04 eV (K) [21,27,32,33]. In Fig. 3c, a significant peak can be observed at around 400.0 eV in the N 1s spectra, which is possibly identified as nitrogen-containing functional group, such as $-C-NH_2$ at 399.56 eV (L) and other substitutional sp^2 nitrogen in the hexagonal rings of a graphene structure at 400.84 eV (M) [27,29,34]. The highest atomic percentage of nitrogen is 4.40% increased from 0% of the control sample (untreated). Finally, in the Fe 2p region, there are two peaks slightly increase which represent to Fe $2p_{1/2}$ (N) and Fe $2p_{3/2}$ (O). The signals in Fe 2p spectra can be allocated to be Fe^0 (before plasma treatment) and Fe_2O_3 and $FeOOH$ (after plasma treatment) [28,31]. This change is the consequence of the carbon etching due to radical and ion bombardment during plasma exposure.

Beside the XPS spectra, the surface analysis of the treated sample is also carried out by the scanning TEM (STEM) image together with an energy dispersive X-ray spectroscopy (EDS) elemental mapping. After taking the STEM images, the EDS elemental mapping can be performed to address the element composition variation in the area of a STEM image. In Fig. 4, the left image (image in white and black color) represents to a STEM image of the treated sample while the four images in the right hand side represent to the EDS elemental mapping of C, Fe, O and N elements, respectively. For example, the map for C element shows the contrast area at the boundary side of particles which correspond to the graphene layers while the map for Fe element shows

the contrast area on the core part of particles which correspond to the iron core nanoparticles. The map of O element has a contrast area in the center of the particle but in less contrast compared to the map of Fe element. It indicates that the oxygen may be mainly found in the iron core nanoparticle rather than on the particle surfaces. On the other hand, the map of N element has a contrast area over the whole area of particles but in less contrast. It indicates that the nitrogen element is found on the whole surface area of the particles, which means that the surface modification successfully attach the nitrogen-containing groups on the outmost of particle surfaces. From the dominant signal at around 399.9 eV in N 1s region found in XPS spectra, it is considered that they are very likely to be amino group.

The proposed mechanism of the nitrogen groups attachment is explained as follows: during the plasma exposure, ion bombardment during the pre-treatment by argon plasma provides a sufficient energy to weaken and break the C–C bonds of the outmost of graphene layer, hence allowing the nitrogen-containing groups formed on the surface of graphene layers after post-treatment of NH_3 plasma. The nitrogen-containing groups formed during the post-treatment plasma selectively attached on the outmost of particle surface (graphene layer). Furthermore, the structural of inner graphene layers and the iron core are still found in stable condition. This means that the ammonia plasma allows the efficient covalent functionalization of nitrogen-containing group to the surface particles without giving any destruction. These features are very analogous to the results of amino group addition on the carbon nanotube by ammonia plasma modification [21].

4. Conclusion

Based on the results and discussion described above, it can be concluded that the graphite encapsulated iron nanoparticles were successfully modified by plasma processing and characterized well using HR-TEM, XPS and EDS with elemental mapping. After the plasma treatment with experimental condition applied here, the surface of the outmost graphene layer was successfully covered by nitrogen-containing groups definitively assigned by XPS spectra and the STEM-EDS elemental mapping. The nitrogen-containing groups formed during the post-treatment plasma selectively attached on the outmost of graphene layer. The inner structure of inner graphene

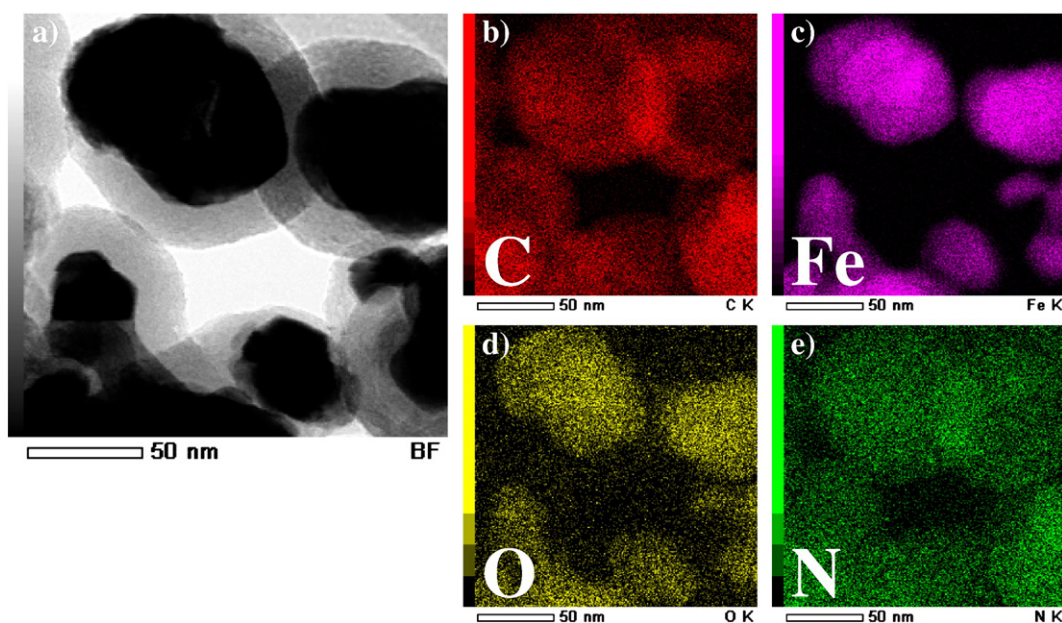


Fig. 4. STEM image (a) and EDS elemental mapping images (b, c, d, and e) of C, Fe, O and N elements, respectively, of treated sample with condition: 10 min of Ar plasma pre-treatment followed by 2 min of NH_3 plasma post-treatment performed at 80 W of RF power and 50 Pa of gas pressure.

layer and the iron core are still found in stable condition which means that the applied plasma condition allows the efficient covalent functionalization of nitrogen-containing group to the surface particles without any destruction.

Acknowledgement

This work has been supported in part by the Grants-in-Aid for Scientific Research and performed under Research and Education Funding for Research Promotion supported by MEXT.

References

- [1] Q.A. Pankhurst, N.K.T. Thanh, S.K. Jones, J. Dobson, *J. Phys. D Appl. Phys.* 42 (2009) 224001.
- [2] C.C. Berry, *J. Phys. D Appl. Phys.* 42 (2009) 224003.
- [3] Q.A. Pankhurst, J. Connolly, S.K. Jones, J. Dobson, *J. Phys. D Appl. Phys.* (2003) R167.
- [4] G. Pastorin, *Pharm. Res.* 26 (2009) 746.
- [5] S. Kim, E. Shibata, R. Sergiienko, T. Nakamura, *Carbon* 46 (2008) 1523.
- [6] A. Ito, M. Shinkai, H. Honda, T. Kobayashi, *J. Biosci. Bioeng.* 100 (2005) 1.
- [7] A.-H. Lu, E.L. Salabas, F. Schuth, *Angew. Chem. Int. Ed.* 46 (2007) 1222.
- [8] C.C. Berry, A.S.G. Curtis, *J. Phys. D Appl. Phys.* (2003) R198.
- [9] R.S. Ruoff, D.C. Lorents, B. Chan, R. Malhotra, S. Subramoney, *Science* 259 (1993) 346.
- [10] M.E. McHenry, S.A. Majetich, J.O. Artman, M. DeGraef, S.W. Staley, *Phys. Rev. B* 49 (1994) 11358.
- [11] Y. Saito, T. Yoshikawa, M. Okuda, N. Fujimoto, S. Yamamuro, K. Wakoh, K. Sumiyama, K. Suzuki, A. Kasuya, Y. Nishina, *J. Appl. Phys.* 75 (1994) 134.
- [12] A.A. Setlur, J.Y. Dai, J.M. Lauerhaas, R.P.H. Chang, *Carbon* 36 (1998) 721.
- [13] Y. Yosida, S. Shida, T. Ohsuna, N. Shiraga, *J. Appl. Phys.* 76 (1994) 4533.
- [14] Y. Saito, T. Yoshikawa, M. Okuda, N. Fujimoto, S. Yamamuro, K. Wakoh, K. Sumiyama, K. Suzuki, A. Kasuya, Y. Nishina, *Chem. Phys. Lett.* 212 (1993) 379.
- [15] M. Nagatsu, T. Yoshida, M. Mesko, A. Ogino, T. Matsuda, T. Tanaka, H. Tatsuoka, K. Murakami, *Carbon* 44 (2006) 3336.
- [16] V.P. Dravid, J.J. Host, M.H. Teng, B.E.J. Hwang, D.L. Johnson, T.O. Mason, J.R. Weertman, *Nature* 374 (1995) 602.
- [17] J. Jiao, S. Seraphin, X. Wang, J.C. Withers, *J. Appl. Phys.* 80 (1996) 103.
- [18] T. Hayashi, S. Hirono, M. Tomita, S. Umamura, *Nature* 381 (1996) 772.
- [19] P.J.F. Harris, S.C. Tsang, *Chem. Phys. Lett.* 293 (1998) 53.
- [20] I.H. Loh, R.E. Cohen, R.F. Baddour, *J. Mater. Sci.* 22 (1987) 2937.
- [21] C. Chen, B. Liang, D. Lu, A. Ogino, X. Wang, M. Nagatsu, *Carbon* 48 (2010) 939.
- [22] A. Felten, C. Bittencourt, J.J. Pireaux, G. Van Lier, J.C. Charlier, *J. Appl. Phys.* 98 (2005) 074308.
- [23] N. Inagaki, K. Narushima, H. Hashimoto, K. Tamura, *Carbon* 45 (2007) 797.
- [24] Z. Remes, A. Choukourov, J. Stuchlik, J. Potmesil, M. Vanecek, *Diamond Relat. Mater.* 15 (2006) 745.
- [25] Z. Remes, A. Kromka, M. Vanecek, A. Grinevich, H. Hartmannova, S. Kmoch, *Diamond Relat. Mater.* 16 (2007) 671.
- [26] W.-K. Oh, H. Yoon, J. Jang, *Diamond Relat. Mater.* 18 (2009) 1316.
- [27] G. Beamson, D. Briggs, *High Resolution XPS of Organic Polymers: The Scienta ESCA 300 Database*, John Wiley & Sons, Chichester, 1992.
- [28] P. Graat, M.A.J. Somers, *Surf. Interface Anal.* 26 (1998) 773.
- [29] K. Schroder, B. Finke, A. Ohl, in: R. D'Agostino, P. Favia, C. Oehr, M.R. Wertheimer (Eds.), *Plasma Processes and Polymers: 16th International Symposium on Plasma Chemistry Taormina, Italy June 22–27, 2003*, Wiley InterScience, Weinheim, 2005, p. 333.
- [30] E. Sosa, R. Cabrera-Sierra, M.T. Oropeza, F. Hernandez, N. Casillas, R. Tremont, C. Cabrera, I. Gonzalez, *Electrochim. Acta* 48 (2003) 1665.
- [31] S. Suzuki, K. Yanagihara, K. Hirokawa, *Surf. Interface Anal.* 30 (2000) 372.
- [32] Z.R. Yue, W. Jjiang, L. Wang, S.D. Gardner, J.C.U. Pittman, *Carbon* 37 (1999) 1785.
- [33] J.-H. Zhou, Z.-J. Sui, J. Zhu, P. Li, D. Chen, Y.-C. Dai, W.-K. Yuan, *Carbon* 45 (2007) 785.
- [34] S. Point, T. Minea, B. Bouchet-Fabre, A. Granier, G. Turban, *Diamond Relat. Mater.* 14 (2005) 891.
- [35] S. Zhang, Y.Q. Fu, X.L. Bui, H.J. Du, *Int. J. Nanosci.* 3 (2004) 797.
- [36] Y.-Q. Wang, H. Viswanathan, A.A. Audi, P.M.A. Sherwood, *Chem. Mater.* 12 (2000) 1100.
- [37] M. Phaner-Goutorbe, *Microsc. Microanal. Microstruct.* 5 (1994) 283.